

Rift Grabens and Crustal Architecture of the Offshore North East Coast-Mahanadi Basin, Eastern Continental Margin of India

Somali Roy, Mainak Choudhuri and Pankaj Gupta

Abstract The rift system in North East Coast-Mahanadi (NEC-MND) basins has been developed during the separation of India and Antarctica, similar to those in Krishna-Godavari (KG) and Cauvery (CY) basins. The rift architecture is well established in the KG and CY basins, both in the onshore as well as offshore. Few publications have reported the presence of rift systems in offshore Mahanadi basin, but very little is known about the continued presence of the rift system to the north of the Mahanadi Basin, in the NEC Basin. The present article has documented the continuation of the rift systems in the offshore NEC Basin, based on interpretation of 2D and 3D seismic reflection data. The internal architecture of the rift grabens have been interpreted and thickness maps been generated to show the distribution of the sediments within the grabens. Seismic velocity data and 2D forward gravity model has also been used to bring out additional informations about the basement and crustal structure.

Keywords India • East coast • Rift • Bengal basin • Mahanadi basin • 3D seismic mapping • RMS amplitude

1 Introduction

Study of coastal tectonics is of interest in regional geoscientific studies (Misra et al. 2014, 2015; Misra and Mukherjee 2015). The North East Coast-Mahanadi (NEC-MND) basin lies in the northern-most part of East Coast of India. Like the Krishna-Godavari (KG) and Cauvery (CY) basins, this basin is also a pericratonic, passive margin basin along the east coast. The wide and stable shelf in this part of the east coast is made up from the heavy discharge of the Ganga-Brahmaputra system in the Bengal basin to the north and from somewhat lesser effects of the rivers like

S. Roy (✉) · M. Choudhuri · P. Gupta
Reliance Industries Limited, Petroleum (E&P), Navi Mumbai, India
e-mail: roysomali29@gmail.com



Fig. 1 Tectonic Evolution of East Coast of India; the figure showing the separation of India and Antarctica around 145 Ma (modified from Reeves 2007, unpublished report for RIL)

Brahmani and Subarnarekha, depositing sediments in and around the study area. The formation of the NEC-MND basin is coeval with that of the KG and CY basins, during the Early Cretaceous breakup between India and Antarctica (Fig. 1), and is well documented in literatures (Rao 2001; Nemčok et al. 2007, 2012). Rift grabens in the onshore NEC-MND area have been documented by Oil India Limited (e.g., Fuloria et al. 1992). The main challenge in this area is to interpret the detailed architecture of rift grabens in the offshore area and continue the structural trend of the basin with other basins in East Coast of India.

The study area lies mostly in the NEC Basin, covering only parts of the Mahanadi basin, between latitude 18.5°N–21.4°N and longitudes 87.2°E–89.5°E (Fig. 2), at water depth between 60 and 2300 m. It is covered by a grid of regional 2D reflection seismic data, with 3D reflection seismic data covering a small part in the NW. Wells drilled by petroleum exploration companies have been correlated and published by Fuloria et al. (1992), which have been considered in the integration of this article. Additionally satellite gravity data is available over the entire area, which has been used to analyze broad basement features. Seismic stacking velocity is available along the seismic data coverage, which is used to clarify the rift signatures in the seismic data.

1.1 Tectonic Framework

The crustal domains along the east coast of India has been taken from Nemčok et al. (2012), where the continent-ocean transition has been divided into a continental-proto-oceanic crust boundary, and a proto-oceanic–oceanic crust boundary, based on interpretations along regional GXT seismic lines and forward gravity modeling.

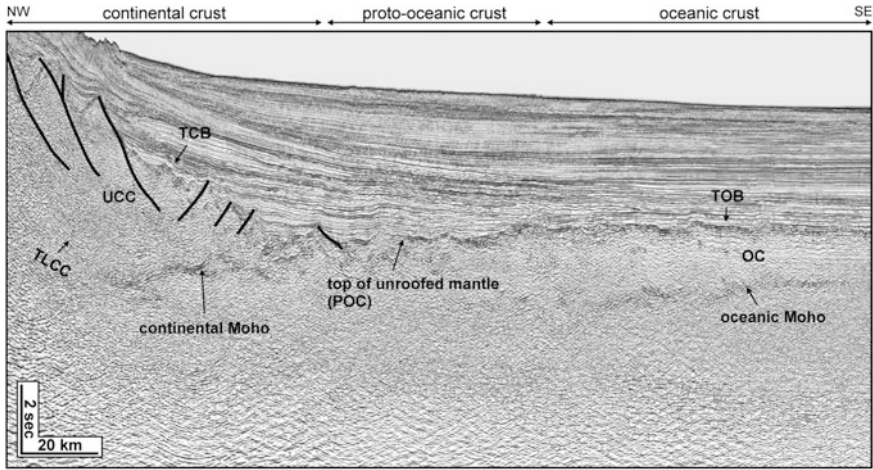


Fig. 3 Seismic line GXT-1000, which runs through the Krishna basin, shows typical section of different crustal types. Nemčok et al. (2012). The line of section is shown in Fig. 2

Their work is mostly concentrated in the KG and CY basins, which has been considered as reference for explaining the structures in the NEC-MND region.

The crustal architecture in the east coast of India is best visualized in the GXT-1000 line in the KG basin, as shown in Fig. 3 (same as Fig. 5 of Nemčok et al. 2012). The figure shows an overall passive margin geometry thinning towards the oceanic side. The presence of rifts in the NW indicates the presence of extended brittle upper continental crust (UCC). The top of basement underneath the sediments is the top of continental basement (TCB). The lower continental crust (LCC) is more ductile than the upper crust, and is shown to contain sub-parallel layering in contrast to chaotic reflections in the UCC; its top is marked as Top Lower Continental (TLCC). Towards SE, the continental crust (CC), eventually, thins out and mantle gets exposed. The exposed mantle in contact with seawater gets serpentinized, forming Proto-Oceanic Crust (POC). The oceanic crust (OC) is formed to the SE of the POC, the top of which is shown as high reflectivity layer termed the top oceanic basement (TOB), while the oceanic Moho is observed below the OC as a diffused layer of higher reflectivity. The CC-POC and POC-OC boundaries from Nemčok et al. (2012) are shown in Fig. 2.

2 Data Used

A synergic approach using reflection seismic data and satellite gravity data has been used to infer the rift signature and crustal domains within the study area.

2.1 Reflection Seismic Data

The multient client GXT IndiaSpan seismic data, acquired by Simpson et al. (2006) for regional geological study in the east coast of India, form the primary seismic database of this study (Fig. 2). Phase I of IndiaSpan covers the entire offshore eastern India and comprises about 13,574 km of 2D data acquisition. It was acquired with a 10 km long offset, 100-fold coverage and 18 s record length and a 2 millisecond (ms) sample rate, with source strength of approximately 200 bar m peak-to-peak power. The imaging depth was about 25 km, which is sufficient to image the entire crust down to Mohorovicic (Moho) discontinuity, together with the different crustal types and their disposition. In the current study, the total data quantum in the east coast of India is 11,587 km (8087 + 3500 km) including both Phase-1 and Phase-1 infill data. The average length of each profile from shelf to ultra-deep water is more than 300 km (Simpson et al. 2006). The data are available in both pre-stack time-(PSTM) and pre-stack depth-migrated (PSDM) formats.

3D seismic data used in this study was recorded by PGS in 2008. 3D seismic is acquired using 6 streamers of 6000 m length and 2 sources (3090 cu in) configuration, which provided surface sampling of 12.5 m along the line and 25 m along the trace. 3D Pre-Stack time migration processing is carried out by WesternGeco. Full fold data covers about 1876 km area and trace length is 9100 ms with 2 ms record length. Stacking velocity information is available at 100 by 100 m grid size.

2.2 Satellite Gravity Data

The study uses public domain satellite free-air gravity anomaly data, available from http://topex.ucsd.edu/WWW_html/mar_topo.html as a global 1-arc minute grid compilation (Sandwell and Smith 2009, V. 20.1). The data is generated by merging marine radar altimetry data from dedicated with EGM2008 global gravity model, available from National Geospatial-Intelligence Agency (NGA), USA, to produce a seamless merged dataset covering the entire Earth. The data is suitable for analysis within a wavelength band of 15–200 km (Sandwell and Smith 1996, 2009) with an error limit of 2–3 mGal (Sandwell and Smith 2009).

The free-air gravity data has been used to create a Bouguer Residual anomaly map using a Bouguer slab density of 2.0 gmcc^{-1} and a 10 km upward continuation filter, to infer the major crustal features, as shown in Fig. 2. Two sharp bands of negative anomaly, separated by a sharp positive anomaly, are observed running parallel to the coastline. The landward band of negative anomaly of about -10 mGal is produced by the rifted half grabens, and the basinward negative band of -10 mGal , adjacent to a positive peak of about 10 mGal , has been interpreted to be due to the crustal transition from continental to proto-oceanic crust. In this data, individual grabens are not clear due to the limited spatial resolution. However there

is a broad zone of low gravity within the 3D area, which is taken to represent the cumulative signature of the grabens in the gravity data. A strike-slip fault, separating the MND and NEC basin, as mentioned by Fuloria et al. (1992) cannot be clearly identified from the gravity anomaly map.

3 Seismic Interpretations

3.1 Crustal Interpretations

An attempt to interpret the crustal domains marking the CC-POC and POC-OC boundaries is made in NEC-MND region as shown in a representative seismic line GXT-1700 that passes through the study area (Fig. 4). In this figure, the TCB and TOB are well observed, as they show higher reflectivity (hard topped) with respect to the sediments above. Though major faults are not observed within the continental crust in this particular seismic section, but some ruggedness are definitely observed which may be formed due to sub-seismic faults and fractures. A subtle reflection is observed below the TCB within thick chaotic reflections, which is interpreted as the TLCC. Moving towards the SE, the continental Moho rises towards the basement top, but is not observed to reach the basement.

The oceanic crustal domain is observed to the SE, with the presence of a well-developed oceanic Moho. The oceanic Moho shows a subtle, but uninterrupted amplitude continuation. The top of oceanic crust is the TOB, with very strong reflection beneath the sediments.

In between the CC and the OC lies a diffused zone without any Moho signature, which has been taken as the POC. The observation is substantiated by the presence of contorted reflections patterns, indicating the deformed nature of this zone, which have been taken as further point in favor of a POC (Karner 2008; Nemčok et al. 2012).

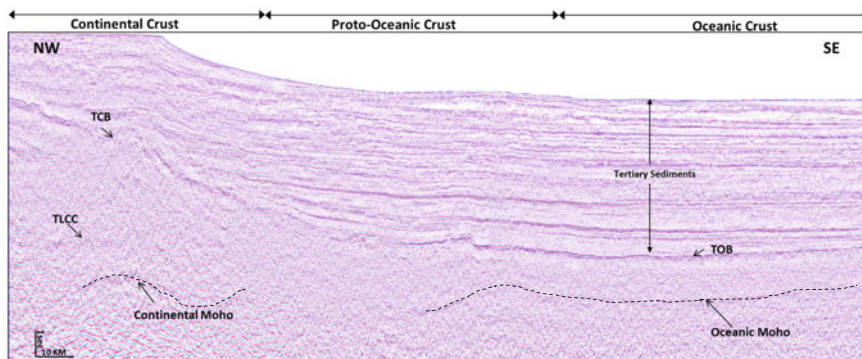


Fig. 4 Regional seismic line GXT-1700 that runs through the study area, north of Mahanadi basin, shows the continental Moho and the oceanic Moho is interpreted at about 11 s

Thus, the ocean-continent transition is interpreted as a diffused zone with two boundaries—(1) a CC-POC boundary, where the upper crust tapers to the surface (though not clearly visible in this section), and it represents the end of the continental crust and (2) a POC-OC boundary defined by the beginning of oceanic Moho and representing the beginning of the oceanic crustal domain. Figure 5 shows the likely position of CC-POC (red cross) and POC-OC (yellow cross) boundaries within the study area as interpreted from the seismic data. The boundaries mapped in the study area shows a landward shift from what interpreted in Nemčok et al. (2012). Further north, the boundaries could not be extended due to absence of deep seismic data.

Figure 5 also shows the position of the extracted profile for gravity modeling and the tentative position of the CC-POC boundary, as discussed later.

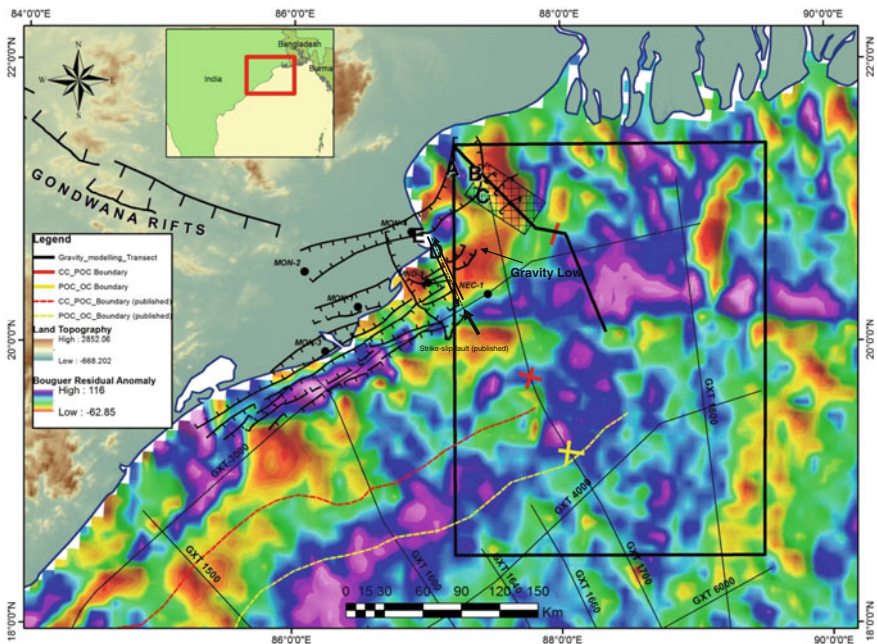


Fig. 5 The zoomed part of Fig. 1. The rift-grabens in the Mahanadi basin are acknowledged from Fuloria et al. (1992). The numbered rift-grabens in the study area are the part of the present paper. The grabens A-C are dipping basinward, whereas the grabens D and E are dipping landward. The black bold line across the grabens A-C is the gravity modeling transect. The red and yellow dashed lines are the CC-POC and POC_OC boundaries respectively from Nemčok et al. (2012). The red and yellow crosses are the interpretations from seismic section Fig. 4. The red line segment on the gravity modeling transect is the CC-POC boundary at a distance of 106.4 km from the beginning of the line. Unroofing of the mantle is not evident in the model, so the boundary is taken at the point where the where the continental crust reached it thinnest. POC-OC boundary is not present in the section, probably is goes through just outside the model limit. The strike-slip fault shown in the figure is taken from Fuloria et al. (1992)

3.2 Rift Signature Interpretation

Seismic mapping has been done for the most prominent reflectors and major chrono-stratigraphic horizons in both the 2D and 3D seismic data. Three major grabens have been identified from 3D seismic data in the northern part of the study area, marked as A, B and C in Fig. 6. The bounding faults of these grabens dip towards the basin margin. Balasore graben is present in the NW as small grabens, with the bounding faults getting reactivated in Tertiary.

For the purpose of establishing the rift architecture, three horizons have been interpreted from 2D seismic data and correlated throughout the study area:

- (a) Basement top (Red horizon)
- (b) Post-rift top (top of rift-related sediments, Yellow horizon)
- (c) Top of Post rift volcanics (Magenta horizon)

The rift packages are identified from their growth geometry towards the bounding fault and truncation at their top at the break-up unconformity. The rift patterns show orientation parallel to the coast line and are related to the India-Antarctica break-up similar to the rift grabens on the adjacent offshore Mahanadi graben and KG and CY basin further south. The mapped synrift base/basement horizon, marked with red color, is shown in Fig. 7a, together with the location of the three main grabens, A, B and C and the Balasore graben towards NW. The colors red-yellow and green-purple in the map indicate lower and higher TWT (two-way-time in milliseconds) values, which represent the shallower and deeper basement depths, respectively. Figure 7b shows the map of the post-rift top, marked

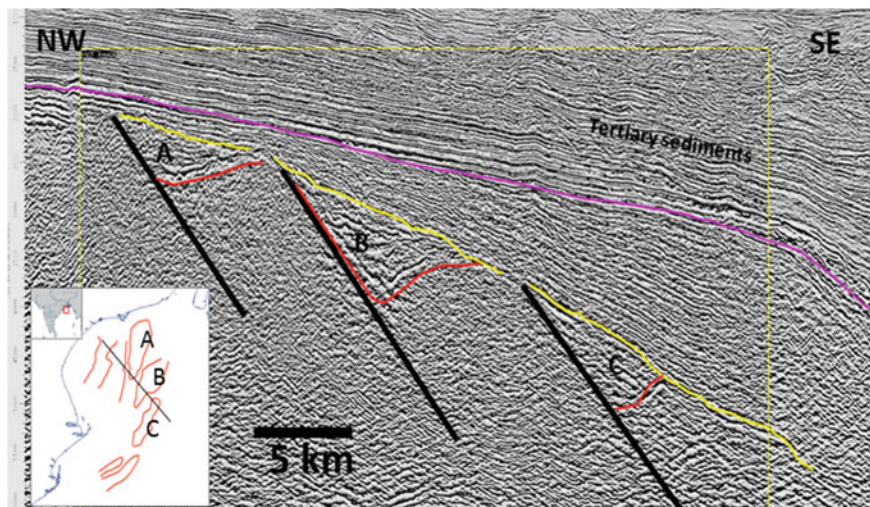


Fig. 6 Seismic section through the study area, showing the key surfaces and the interpreted grabens. Vertical scale is in ms TWT (two-way-time)

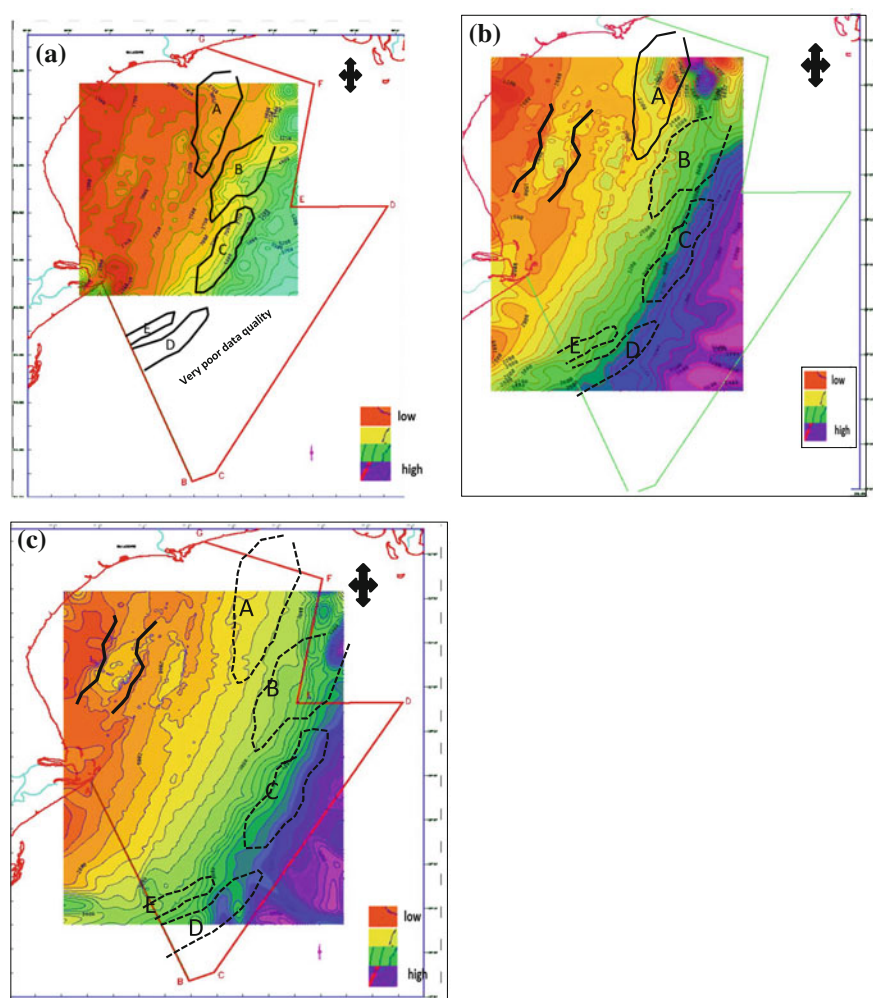


Fig. 7 **a** TWT structure map of basement top (syn-rift base) in the study area. The colours *red* and *yellow* are low values and *blue* and *purple* are high values. The data quality of 2D seismic lines are very poor, thus the map could not be extrapolated till grabens D and E. **b** TWT structure map of post-rift top in the study area. **c** TWT structure map of top of post-rift volcanics

with yellow in Fig. 6. The graben geometry is difficult to identify from this map, except for graben A. Figure 7c shows the map of the post-rift volcanics, with the topography mimicking the present day sea floor.

Five 2D seismic profiles are shown for details of the individual grabens in the NEC-MND basin (Figs. 8, 9, 10, 11 and 12), together with the interpreted key seismic reflectors. Figure 8 shows the grabens A and B; graben B is further subdivided into B' and B'', based on a subsidiary fault within the main depocentre. In this and the subsequent figure, the reflectors below the red horizon are chaotic in

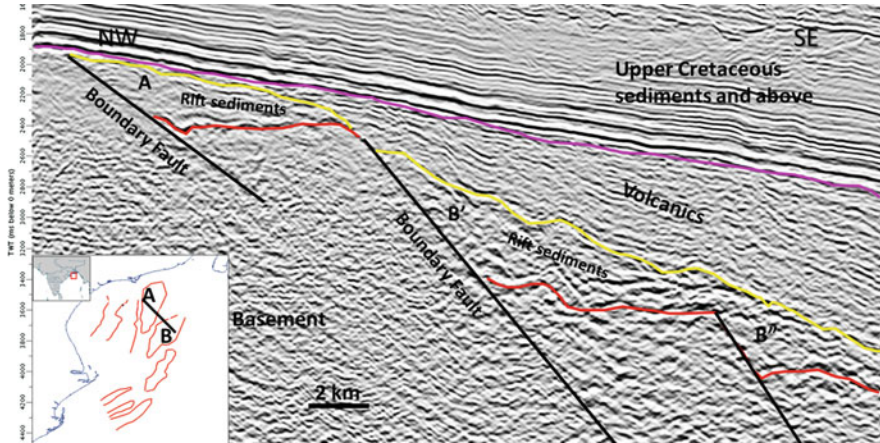


Fig. 8 Seismic section through the study area, showing the key surfaces and the interpreted grabens. Vertical scale is in ms TWT

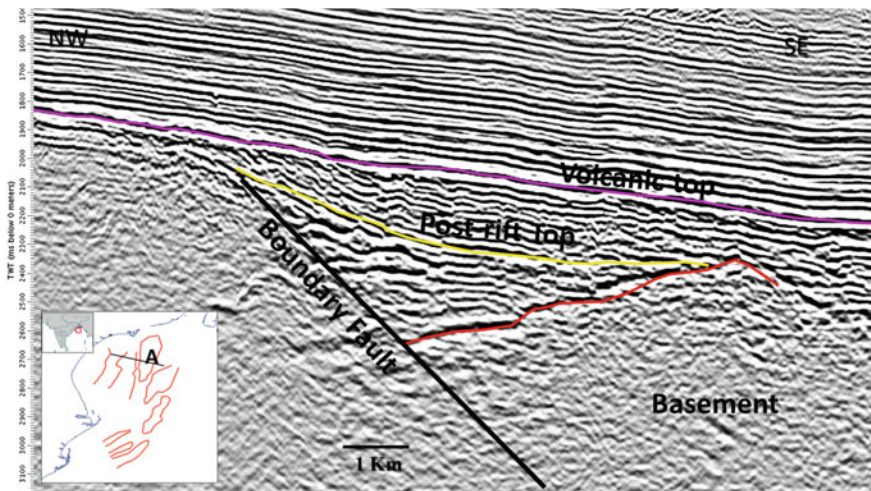


Fig. 9 Seismic section through the study area, showing the key surfaces within graben A. Vertical scale is in ms TWT

nature and show no proper pattern, and are interpreted as the basement. Seismically similar correlatable package has been drilled by OIL and ONGC Ltd. in MON-4 (onland) and MND-1(offshore) in Mahanadi basin, indicating the presence of basement. Thus the red horizon is interpreted as the basement top. The black lines are the faults observed within the basement. The reflectors above the red horizon show growth patterns typical of synrift package. The top of this sediment package is the yellow horizon above which no growth patterns are observed. Above the synrift package (yellow horizon), show bright amplitude and low frequency, and are

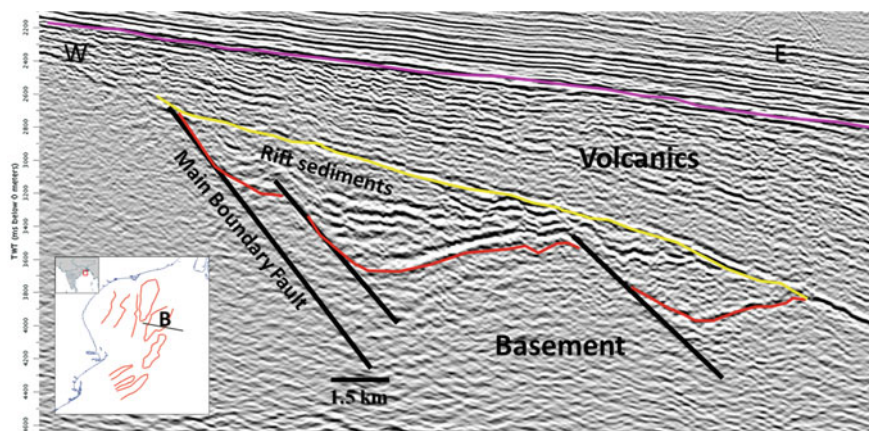


Fig. 10 Seismic section through the study area, showing the key surfaces for Graben B. Vertical scale is in ms TWT

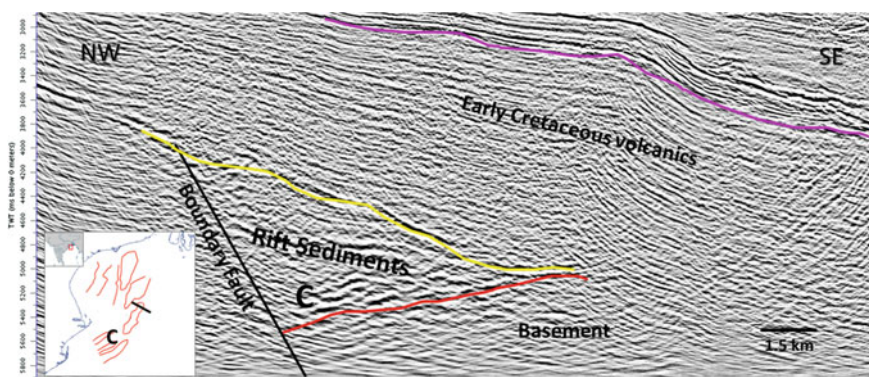


Fig. 11 Seismic section through the study area, showing the key surfaces for Graben C. Vertical scale is in ms TWT

interpreted as lava-flows. This package has been drilled in the offshore well NEC-1, whose location is shown in Fig. 5, in other part of Mahanadi basin, confirming the lithology. These lava flows are probably related to late Early Cretaceous volcanism associated with Rajmahal traps and 85°E Ridge volcanism, based on similar time of formations (Bakshi 1995) and geographical closeness. The palynological assemblage recorded in these basalts is related to Rajmahal Traps and 85°E Ridge which is reported by Interra Exploration Company (India) Private Ltd. Figures 9, 10 and 11 show the geometry of the individual grabens A, B and C in detail. Note that in Fig. 11, the Early Cretaceous volcanics become thicker on top of graben C, which lies more towards the CC-POC boundary, compared to that in grabens A and B. Apart from the major grabens, A, B and C, two minor grabens, D and E lies outside

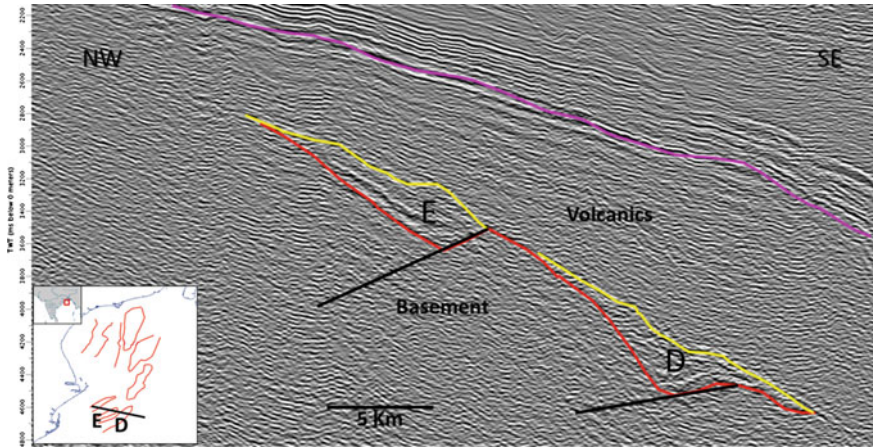


Fig. 12 Seismic section through the study area, showing the key surfaces for grabens D and E. Vertical scale is in ms TWT

the 3D area, in the southern part of the study area (Fig. 12). The bounding faults in these grabens dip landwards.

3.2.1 3D Seismic Mapping

3D seismic data enables us to identify the sedimentation history within the synrift grabens in much detail, and consequently, four horizons have been mapped within the synrift packages from in 3D seismic volume as shown in Fig. 13:

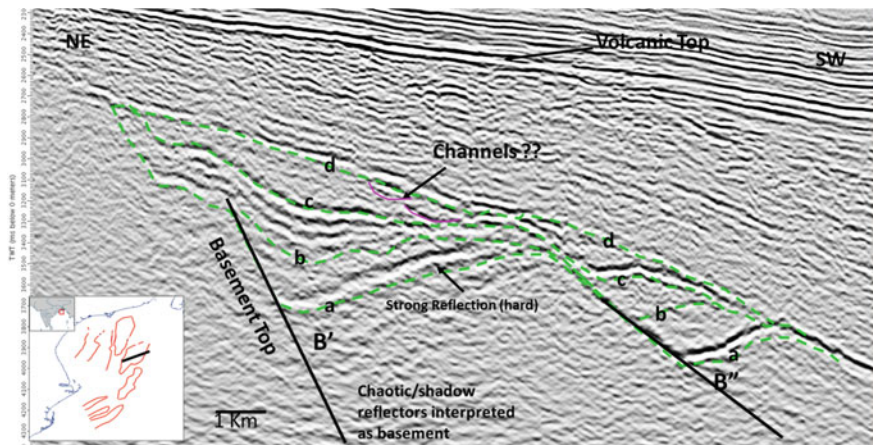


Fig. 13 The figure showing the detailed interpretation in an arbitrary line across the graben B in TWT (ms)

- (a) Syn-rift base (Basement top)
- (b) Early Synrift top
- (c) Late Synrift top (Synrift top)
- (d) Sag phase top (Post-rift top)

The horizons mapped from the 3D seismic data are present locally and we have not been able to correlate them across the different grabens. An illustrated example of these subdivisions of the synrift package has been shown for graben B, whose seismic imaging is better than those of grabens A and C. Figure 13 shows an arbitrary seismic profile across graben B with the horizons interpreted in 3D seismic volume. The reflector 'a' is very prominent and it demarcates the interface between the chaotic reflectors below and the wedge forming reflectors above. Thus the reflector 'a' indicates the basement top. The top of 'a' shows wedge-pattern reflectors with thickening sediments near the faults marked in black, indicating growth pattern characteristics of synrift deposits. This sediment package shows an absence of layering and reflection continuity, and is indicative of sudden influx of locally derived sediments within the synrift, probably representing alluvial fans and fan deltas. This may indicate the beginning of syn-rift phase, the top of which, and reflector 'b'; is taken as the end of early rift sedimentation. The reflectors above 'b' show high reflectivity with parallel sediment patterns, typical of calm lacustrine environment (Morley and Wescott 1999), the top of which is marks the end of synrift sedimentation, and is indicated by the reflector 'c'. The reflectors above 'c' are parallel to sub-parallel and also show concave-up reflections indicative of local accommodation during post rift sedimentation, and are taken to represent sag-phase deposits. The reflector 'd' mark the top of the sag phase post-rift sediments. Above the sag phase deposits, the reflectors are of high amplitude and low frequency, with some chaotic patters, and are taken to represent the Early Cretaceous volcanics, as discussed in the earlier section.

Figure 14a shows the time-structural map of horizon 'a' at the synrift base. In this figure, two grabens are observed: B' and B'', along which the accommodation spaces are created during various phases of rifting. These are individual rift systems having their respective basin bounding faults forming two isolated basins. The dimension of graben B' is larger than that of B''. The overall extents of the rift grabens are unknown due to limited data extent. Figure 14b, shows the 3D perspective view of the same time structure map.

Figure 15a shows the time-structure map of horizon 'c' at the top of synrift. Figure 15b, shows the RMS (Root Mean Squared) amplitude map of the late synrift top. The red dashed boundary marked around the high amplitude response shows a narrow head and broaden end, and may represent a lobate feature associated with a channelized flow system. The direction of the flow is orthogonal to the fault displacement.

Figure 16a shows the time-structure map of horizon 'd', the top-most horizon in the rift basin marking the end of sag phase sedimentation. Figure 16b shows the RMS amplitude map of the same, extracted in a window along the horizon with

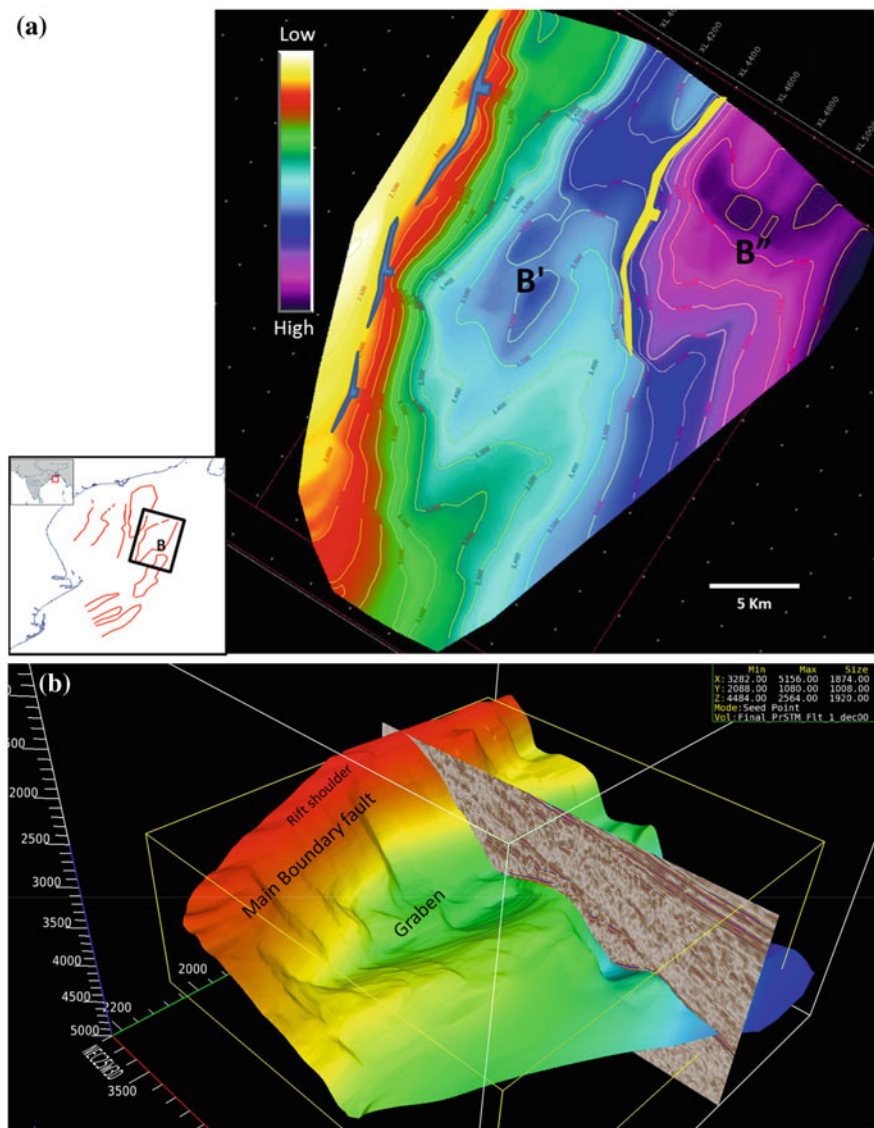


Fig. 14 **a** Time-structure map view of the base of synrift. **b** 3D view of base of the synrift base. Red and yellow colours show shallow depth and green and blue colours show deeper depth

30 ms top and below to it. The high amplitude in the figure may indicate the presence of coarse-grained sediments.

Figure 17 shows the TWT thickness map between the synrift base and the synrift top. In this figure some prominent depocentres are present, corresponding to the grabenal geometry. The thickest sediments are along the bounding faults, indicating growth nature of the fills.

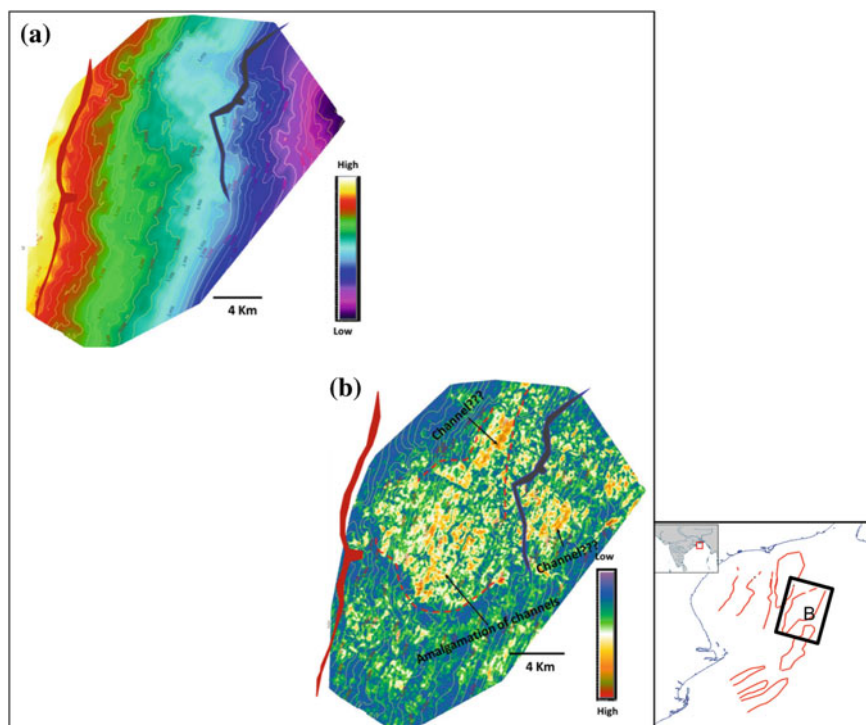


Fig. 15 **a** Time structure map of top of early syn-rift phase; **b** amplitude map overlaid by TWT contours. The location of the maps is shown in the *inset*

Seismic velocity analysis has been performed to support the interpreted graben geometry, which shows a good fit with the interpretation. Figure 18 is a representative velocity profile along graben B, illustrating the fit between the interpretation and velocity variation. Major velocity change is seen at the interpreted basement level where velocity reaches more than 5500 m/s. Figure 19 shows a time-vs-velocity plot along a 1D location shown with dashed line in Fig. 18. It shows that the interval velocity ranges between 4900 and 5400 m/s within the synrift sequence, and increases drastically within the basement. The sediments within post-rift sequence shows a slight velocity inversion, which then increases again within the synrift.

3.3 2D Forward Gravity Modeling

2D forward gravity modeling has been used to validate the interpreted crustal boundaries from seismic data. It involves setting up a model, calculating the gravity anomaly, comparing it with the observed data and iteratively varying the density of

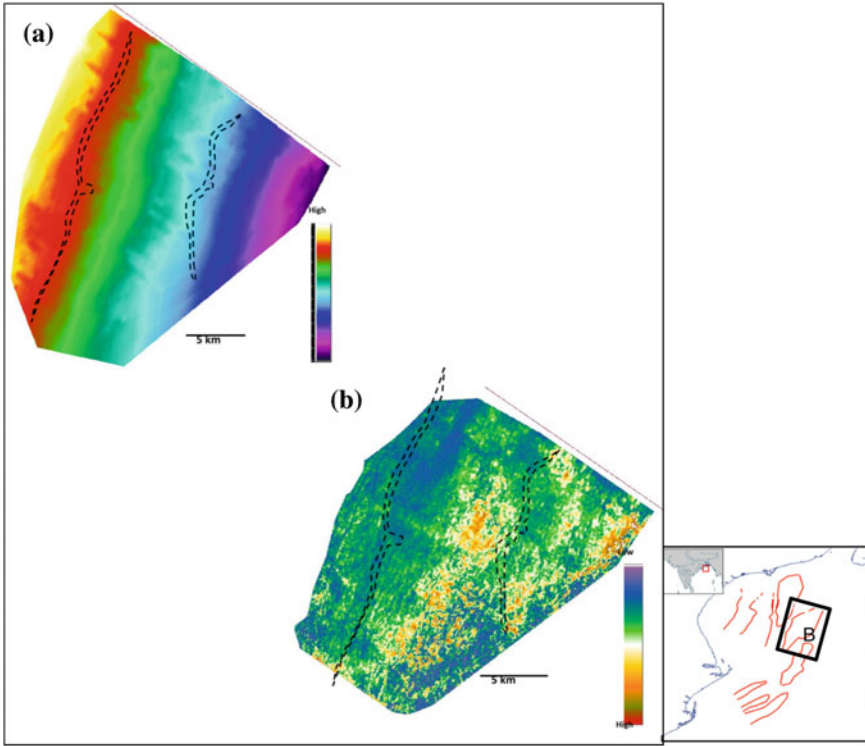


Fig. 16 **a** Time structure map of top of late syn-rift phase; **b** amplitude map of the syn-rift top

the interpreted layers and modifying the source body geometries until the calculated anomaly matches well with the observed data. The modeling is done in GM-SYS 5.01.10, which is part of Geosoft's Oasis montaj 6.4.2 suite. The densities used for the different layers (e.g. Clark 1966; Touloukian et al. 1981; Christensen and Mooney 1995; Lillie 1999) are shown in Table 1. The software calculates the gravity anomaly response, which is matched with the observed data and a difference is calculated, which needs to be minimized to get a good fit. The methods used to calculate the gravity model response is based on the methods of Talwani et al. (1959), and make use of the algorithms described in Won and Bevis (1987). All the models extend to $\pm 30,000$ km in the $-X$ and $+X$ directions to eliminate edge-effects.

The free-air gravity anomaly includes the gravity effect of the water layer at the water-sediment interface, and shows a strong correlation with bathymetry. In the current study, a profile extracted from the gravity anomaly data is used to interpret the crustal geometry in the study area and is validated by forward gravity modeling. As the seismic section along the extracted profile is only 13 km deep (check depth), the crustal layers were all interpreted based on gravity signature, the last seismically interpreted horizon being the Lower Cretaceous volcanic base over the synrift

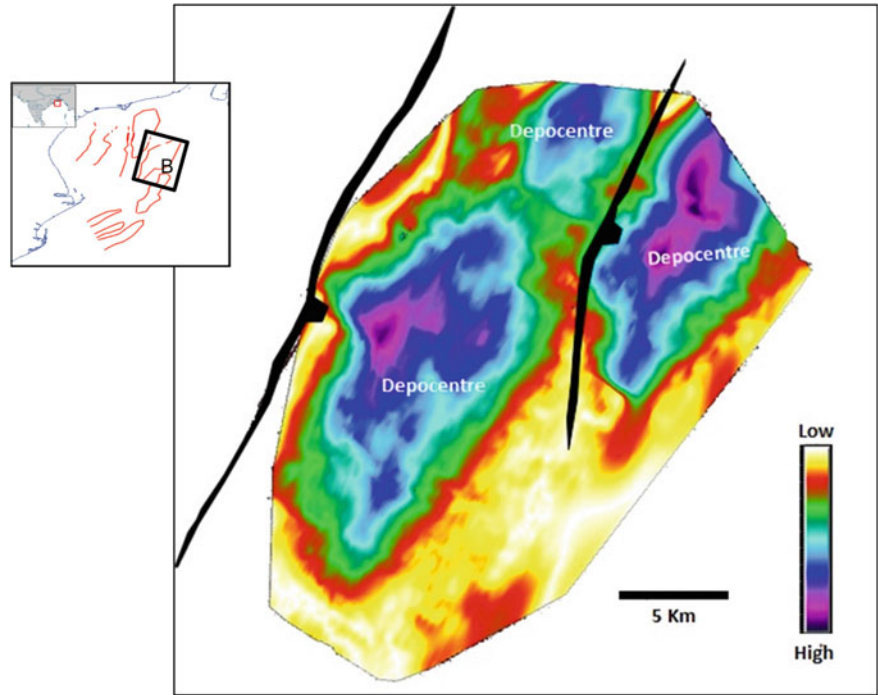


Fig. 17 The figure showing the TWT thickness map (ms) between the Synrift base and the Synrift top

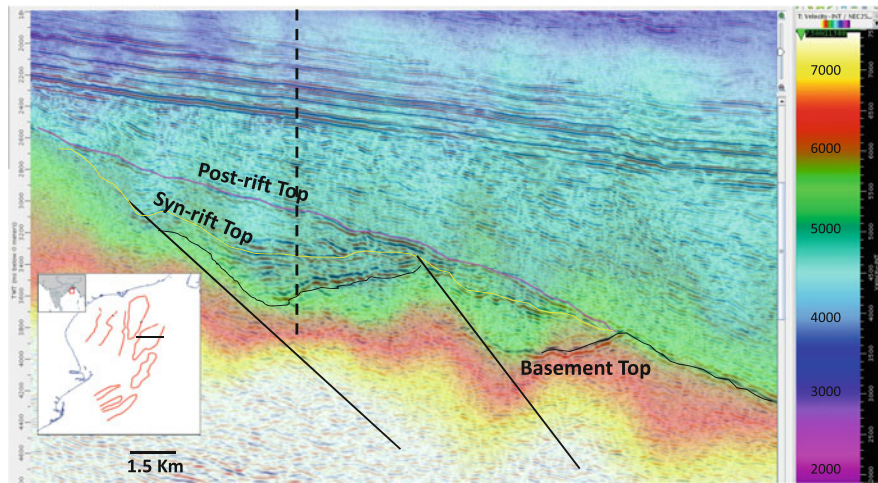


Fig. 18 The figure showing the seismic section overlaid by interval velocity. The *dashed line* is the location for 1D-profile in Fig. 19

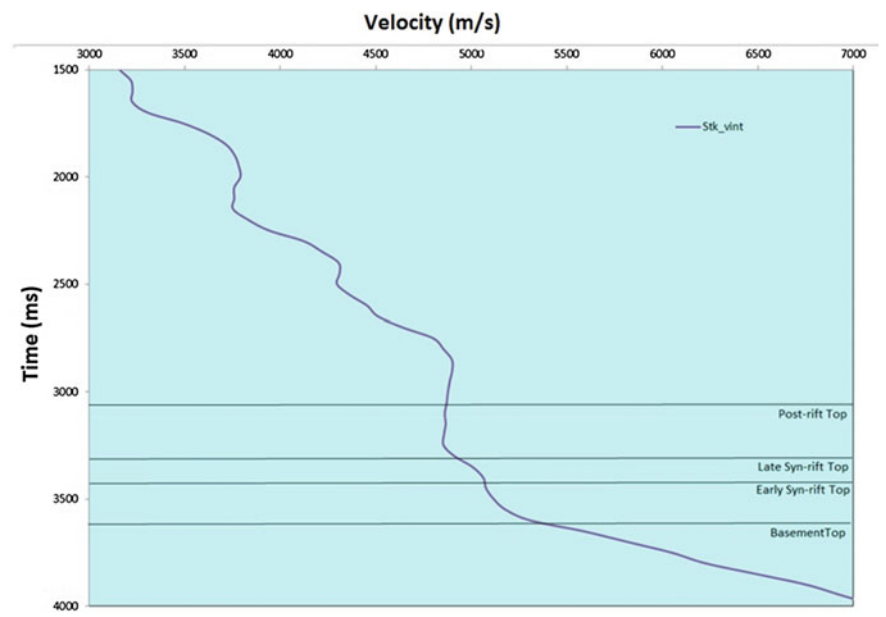


Fig. 19 The figure showing the interval velocity plot at the graben B (the location is shown as dashed line in Fig. 18)

Table 1 Densities used in gravity modeling

| Layer | Density (g cm ⁻³) | Type |
|--------------------|-------------------------------|-----------|
| Water | 1.03 | Water |
| Sediment 1 | 2.3 | Sediment |
| Sediment 2 | 2.4 | |
| Sediment 3 | 2.5 | |
| Sediment 4 | 2.6 | |
| Volcanics | 2.7–2.9 | Volcanics |
| Upper cont. crust | 2.63 | Crust |
| Middle cont. crust | 2.89 | |
| Lower cont. crust | 3.04 | |
| Upper ocn. crust | 2.7 | |
| Middle ocn. crust | 2.89 | |
| Lower ocn. crust | 3.04 | |
| Mantle | 3.36 | Mantle |

Cont—continental and ocn—oceanic

grabens. Gravity data has also been used to check for the presence of low density synrift sequences below the basalt, but because of small dimensions of the individual grabens compared to the spatial resolution of the data points, it was not possible to uniquely isolate the gravity signature of the grabens. The extracted

profile shows moderate negative values between -25 and -45 mGal in the continental side, gently rising to $+45$ mGal near the shelf break and then rapidly falls to -8 mGal as the basin deepens.

During forward gravity modeling, different models have been tried to match the observed gravity anomaly, and the one that fits the expected crustal architecture in the study area (Nemčok et al. 2007, 2012; Sinha et al. 2010) has been taken. The modeled profiles (Figs. 20, 21 and 22) whose location is shown in Fig. 5 show a thinning of the continental crust towards the basinal side, gradually merging with oceanic crustal rocks, without any definite presence of exhumed mantle zone. This is expected in regions affected by post-rift volcanism, where the gravity signature of the unroofed Moho gets lost in the voluminous magma flows. The same is observed in Fig. 4, where the basinward termination of the continental Moho is unclear, leaving doubt about unroofed mantle. The shallowest mantle comes up at a gravity

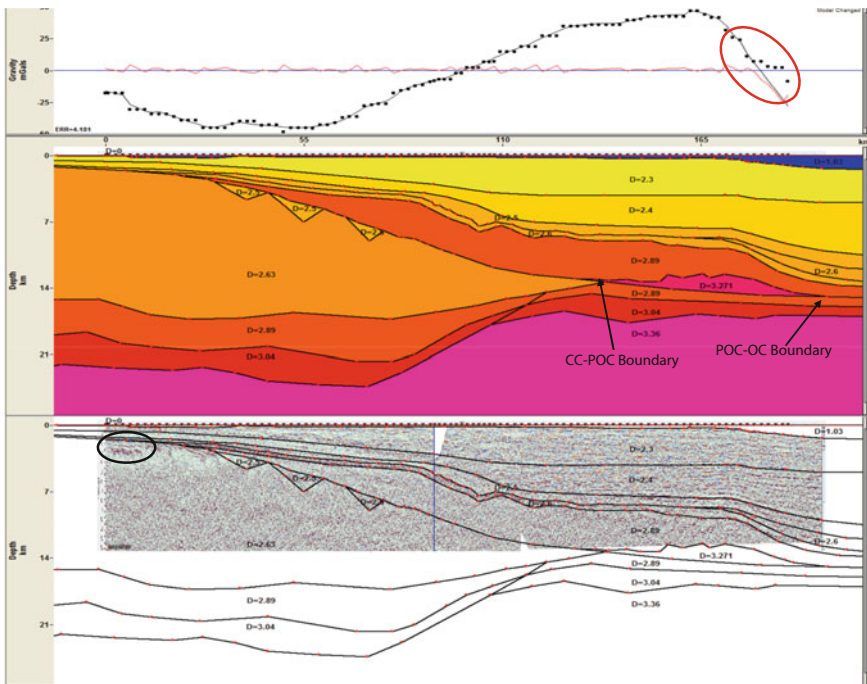


Fig. 20 Forward gravity model along profile extracted across the NEC basin, showing a good match between the observed and calculated gravity anomaly values. The blocks with prescribed density are matched with the seismic interpretation of the main boundaries to prepare the model. *Dotted line*—observed gravity anomaly values, *thin line*—calculated values, *red line* along zero mGal—difference between observed and calculated anomaly values. The extreme end of the data shows a sharp lowering of gravity anomaly value (*red circle*), which has not been modelled. The basinward gravity anomaly high has been explained by the presence of a high density body (of 3.2 g cm^{-3}) below the basalt flows which may represent an intrusive body. Balasore graben is marked in *black*

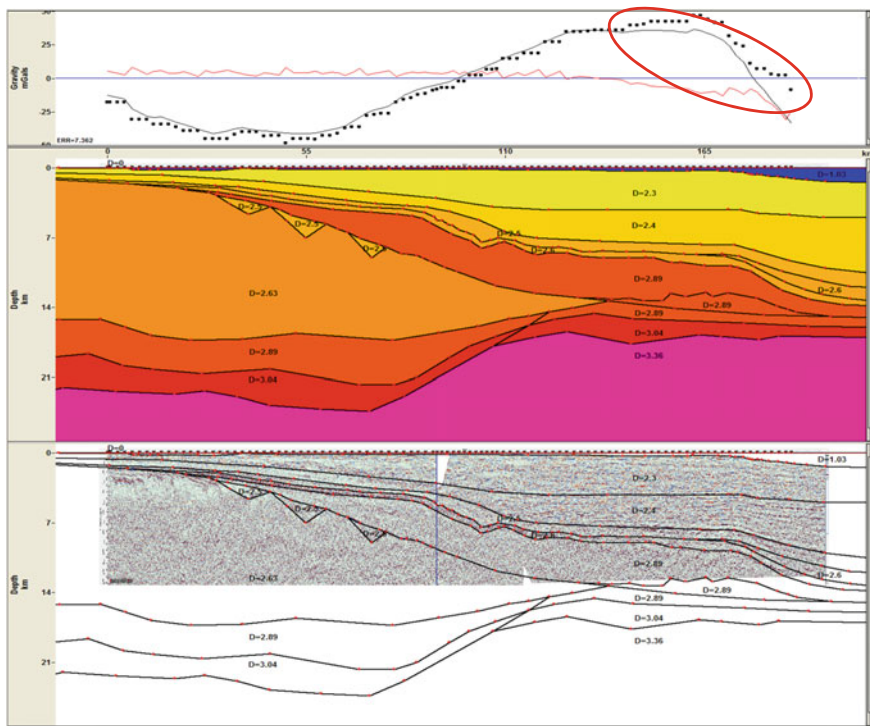


Fig. 21 Same as Fig. 20. Changing the density of the high density body to match that of the basalt/middle crust immediately shows up as a strong localized decrease of the modelled gravity anomaly values (circled red)

anomaly value of +33 mGal, while further rise in gravity anomaly requires the inclusion of a high density body (of 3.2 g cm^{-3}) below the basalt flows which may represent an intrusive body (Fig. 20). With the absence of this high-density layer, a strong localized decrease of the modeled gravity anomaly values is observed on the basinward side of the profile (Fig. 21). The extreme basinward end of the data shows a sharp lowering of gravity anomaly values, which from its frequency content, seems to be a shallow level density anomaly within the sedimentary layers, or at the water-sediment interface. It has not been modeled in this study. The synrift grabens observed in seismic image has been assigned a density of 2.5 g cm^{-3} , which when removed shows a negligible change in the calculated gravity anomaly sharing that the spatial resolution at the gravity data is insignificant to properly model the synrift grabens (Fig. 22).

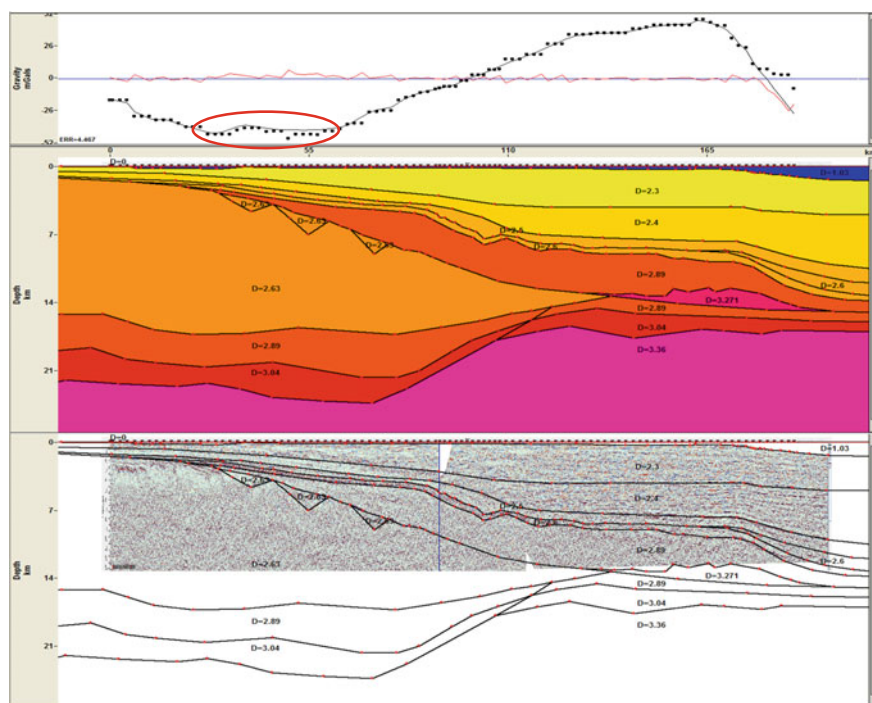


Fig. 22 Same as Fig. 20. Changing the density of synrift grabens to match that of the *upper* continental crust shows up as a gentle increase in the calculated gravity anomaly (*circled red*)

4 Discussions on Synrift Age

The interpretation of rift grabens below Early Cretaceous volcanics has been reported for the first time from the study area. The three major grabens are small and isolated, and may represent the distal end of the rifted continental crust. The rift age is not available in this region. The rift age, as determined biostratigraphically in the Krishna-Godavari basin is from Toarcian to Valanginian. In NEC-MND basin, the rift age is uncertain mainly because of ambiguity between well data (ONGC and OIL drilled wells) and the biostratigraphic report (Interra Exploration Company (India) Private Ltd.) and the absence of seismic data correlating these wells. RIL has not drilled any well in these rift grabens. Four onland wells, earlier drilled by OIL in the grabens shown in Fig. 2 have reported Early Cretaceous as the age of the oldest sediments in these grabens (Fuloria et al. 1992). RIL's in-house interpretations suggest that the synrift sediments drilled in MON-4 and MND-1 well are of Upper Jurassic age, based on the presence of *Callialasporites dampieri*, a key marker of Jurassic age. Further support comes from Adyalkar (1964), who suggest a Liassic age (Lower Jurassic) for the outcrops of Atgarh sandstone near Cuttack, Orissa, believed to be of syn-rift deposits related to India-Antarctica break-up.

5 Conclusions

Based on the above interpretations and discussions the following points have been concluded:

1. The rift system has been observed in the NEC-Mahanadi basin, whose orientation is inline with the rift systems seen in KG and CY basins.
2. Due to limited data control, the CC-POC and POC-OC boundaries can only be interpreted in GXT-1700.
3. The actual presence of a strike slip fault between Mahanadi and NEC rift grabens as mentioned in Fuloria et al. (1992), could not be established from our current dataset.
4. The sedimentary sequences within the synrift succession points towards a well-developed synrift system in the NEC-Mahanadi basin.
5. The presence of rifts in the basin cannot be interpreted from 2D Gravity modelling.

Acknowledgments The article is derived from Reliance's internal report on new play prospectivity in the NEC basin as part of RIL's new opportunity screening. The authors thank Reliance Industries Ltd. for allowing them to publish the results of this study.

References

- Adyalkar P (1964) Sedimentological study of the Atgarh sandstones. Cuttack district, Orissa
- Bakshi AK (1995) Petrogenesis and timing of volcanism in the Rajmahal flood basalt province, northeastern India. *Chem Geol* 73–90
- Christensen NI, Mooney WD (1995) Seismic velocity structure and composition of the continental crust: A global overview. *J Geophys* 9761–9788
- Clark SP (1966) Handbook of physical constants. *Geol Soc Am Mem* 587
- Fuloria R, Pandey R, Bharali B, Mishra J (1992) Stratigraphy, structure and tectonics of Mahanadi offshore basin. *Geol Surv Ind Spec Publ* 29:255–265
- Interra Exploration Company (India) Private Ltd. (n.d.). Structural and stratigraphical interpretation of geological and 2D seismic data NEC block, Mahanadi offshore. Interra Exploration Company (India) Private Ltd, Mumbai
- Karner GD (2008) Depth-dependent extension and mantle exhumation: an extreme passive margin end-member or a new paradigm? In: Central atlantic conjugate margin conference. Halifax, Canada
- Lillie RJ (1999) Whole earth geophysics: an introductory textbook for geologists and geophysicists, 1st edn. Prentice Hall, Upper Saddle River, pp 251–277
- Misra AA, Bhattacharyya G, Mukherjee S, Bose N (2014) Near N–S paleo-extension in the western Deccan region, India: Does it link strike-slip tectonics with India–Seychelles rifting? *Int J Earth Sci* 103:1645–1680
- Misra AA, Mukherjee S (2015) Tectonic inheritance in continental rifts and passive margins. *SpringerBriefs in Earth Sciences* (in Press)
- Misra AA, Sinha N, Mukherjee S (2015) Repeat ridge jumps and microcontinent separation: insights from NE Arabian Sea. *Mar Pet Geol* 59:406–428

- Morley CK, Wescott WA (1999) Sedimentary environments and geometry of sedimentary bodies determined from subsurface studies in East Africa. *AAPG Stud Geol* 44:211–231
- Nemcok M, Sinha S, Stuart C, Welker C, Choudhuri M, Sharma S et al (2012) East Indian margin evolution and crustal architecture: integration of deep reflection seismic interpretation and gravity modeling. Geological Society, London, Special Publications, London
- Nemcok M, Stuart C, Welker C, Smith S, Yalamanchili S, Srivastava DC et al (2007) Crustal types, structural architecture and plate configurations study of Reliance east coast region. EGI for Reliance Industries Limited, Navi Mumbai
- Rao GN (2001) Sedimentation, stratigraphy, and petroleum potential of Krishna-Godavari basin, east coast of India. *Am Assoc Pet Geol* 85:1623–1643
- Sandwell DT, Smith WF (1996) Global bathymetry prediction for ocean modeling and marine geophysics. http://topex.ucsd.edu/marine_topo/text/topo.html
- Sandwell DT, Smith WF (2009) Global marine gravity from retracked Geosat and ERS-1 altimetry: ridge segmentation versus spreading rate. *J Geophys* 114 B01411
- Simpson K, Plummer J, Brink R (2006) Report on contractor performance during the ‘INDIASPAN’ 2D marine seismic reflection survey offshore India. Survey by Scan Geophysical ASA onboard the M/V Geo Searcher for GX Technology Corporation
- Sinha ST, Nemcok M, Choudhuri M, Misra AA, Sharma SP, Sinha N et al (2010) The crustal architecture and continental break up of East India passive margin: an integrated study of deep reflection seismic interpretation and gravity modeling. AAPG Annual Convention & Exhibition, New Orleans
- Talwani M, Heirtzler JR (1964) Computation of magnetic anomalies caused by two dimensional bodies of arbitrary shape. In: Parks GA (ed) *Computers in the mineral industries*, part 1, Stanford University. Publications, Geological Sciences, pp 464–480
- Talwani M, Worzel JL, Landisman M (1959) Rapid gravity computations for two dimensional bodies with application to the Mendocino submarine fracture zone. *J Geophys Res* 64:49–59
- Touloukian YS, Judd WR, Roy RF (1981) *Physical properties of rocks and minerals*. McGraw-Hill, New York, pp 230–411
- Won IJ, Bevis M (1987) Computing the gravitational and magnetic anomalies due to a polygon: algorithms and fortran subroutines. *Geophysics* 52:232–238

Petroleum Geosciences: Indian Contexts

Mukherjee, S. (Ed.)

2015, VI, 294 p. 127 illus., 113 illus. in color., Hardcover

ISBN: 978-3-319-03118-7